Effect of Variation of Portal Venous Blood Flow on Radiofrequency and Microwave Ablations in a Blood-perfused Bovine Liver Model[1]

Gerald D. Dodd III, MD
Nicholas A. Dodd, BPA
Anthony C. Lanctot, MS
Deborah A. Glueck, PhD

Purpose: To assess whether there is a significant difference in the effect of incremental changes of portal venous blood flow rates on the size of radiofrequency (RF) versus microwave (MW) ablation lesions in an ex vivo blood-perfused bovine liver model.

Materials and Methods: This study was exempt from approval by the Institutional Animal Care and Use Committee. Sixty ablations (30 MW and 30 RF ablations) were performed ex vivo in 15 bovine livers perfused with autologous blood via the portal vein at 60, 70, 80, 90, and 100 mL/min per 100 g of liver tissue (three livers were used for each flow rate). Long-axis diameter (LAD), short-axis diameter (SAD), and volume were measured for each ablation lesion. A general linear mixed model was used to examine the effect of location, ablation device, and flow rate on LAD, SAD, and volume. Results were considered to indicate a significant difference at P less than .05.

Results: Location was not a significant predictor of LAD, SAD, or volume ($P \geq .4$). The slope of the relationship between flow rate and LAD, SAD, and volume was significantly different according to ablation device ($P < .0001$). For RF ablation lesions, the mean LAD, SAD, and volume demonstrated a significant inverse relationship with flow rate, while the measurements for MW ablation did not change with variation in flow rates.

Conclusion: The size of RF ablation lesions is highly variable, with a significant inverse relationship to the rate of portal venous blood flow. Conversely, the size of MW ablation lesions is unaffected by changes in portal venous blood flow. The consistency of the size of MW ablation lesions could translate into a higher local tumor eradication rate than that reported with RF ablation.

[1] From the Department of Radiology, School of Medicine (G.D.D., N.A.D., A.C.L.) and School of Public Health (D.A.G.), University of Colorado, Mail Stop L954, 12401 E 17th Ave, PO Box 6510, Aurora, CO 80045. Received March 7, 2012; revision requested May 22; revision received June 29; accepted July 25; final version accepted September 27. Supported in part by the National Science Foundation, grant no. HRD-0932339, and by a grant from BSD Medical, Salt Lake City, Utah. **Address correspondence to** G.D.D. (e-mail: *gerald.dodd@ucdenver.edu*).

Radiofrequency (RF) ablation is a widely accepted technique for treating primary and secondary malignant hepatic tumors (1–4); however, its success rate in eradicating tumors is affected by multiple factors, including tumor size and location, hepatic blood flow, equipment, and technique (5–7). Of these, hepatic blood flow is a perplexing variable that has been shown to have a substantial effect on the success rate of local tumor eradication. Multiple studies have shown that the size of RF ablation lesions is inversely related to hepatic blood flow. An increase or decrease in global or regional hepatic blood flow causes an inverse change in the overall size of RF ablation lesions (8–22). While RF ablation systems can create ablation lesions up to 7 cm in diameter, the intrinsic variability in hepatic blood flow between individuals and within the same person limits the average effective ablation size of RF ablation devices to approximately 3.5 cm (23–27). This limited effective size is directly related to the high success rate (>90%) reported for eradication of tumors smaller than 3 cm and the precipitous decrease in success rate for larger tumors (1–6).

Microwave (MW) ablation devices are an attractive alternative to RF ablation devices, in part because of a diminished susceptibility to the "heat sink" effect (local cooling of thermal process) caused by adjacent hepatic blood vessels (28–32). In studies of the heat sink effect on MW ablation, the coagulative necrosis is either unaffected or minimally indented in the region immediately contiguous to large blood vessels. Histologic analysis of MW ablation lesions demonstrates complete coagulation necrosis of tissue down to and even enveloping blood vessels as large as 11 mm in diameter. While these data are very encouraging, there is conflicting information regarding the effect of alterations of global or regional hepatic blood flow on the size of MW ablation lesions. Investigators of various studies report that the size of coagulation necrosis is unaffected, increased, and decreased by the presence of hepatic blood flow (33–38). Furthermore, these investigators looked only at the effect of the presence or absence of flow, and none addressed the important issue of the effect of incremental changes in hepatic blood flow rate on the size of MW ablation lesions.

Given the importance of accurate performance characteristics of MW ablation devices on the success rate of liver tumor ablation, we performed a study to assess if there is a significant difference in the effect of incremental changes of portal venous blood flow rates on the size of RF versus MW ablation lesions in an ex vivo blood-perfused bovine liver model (39).

Advance in Knowledge

- The size of radiofrequency (RF) ablation lesions is highly variable (volume, 3.7–12.5 cm^3), with a significant ($P < .05$) inverse relationship to the rate of portal venous blood flow; conversely, the size of microwave (MW) ablation lesions is essentially unaffected by changes in portal venous blood flow.

Implication for Patient Care

- The consistency of the size of MW ablation lesions could translate into a higher local tumor eradication rate than that reported with RF ablation.

Materials and Methods

This study was exempt from approval by our Institutional Animal Care and Use Committee. It was supported in part by the National Science Foundation, grant no. HRD-0932339, and by BSD Medical (Salt Lake City, Utah), which provided funding and equipment. The entire experiment, including design, study execution, data collection, data analysis, and manuscript preparation, was under the control of and performed by the authors. None of the authors are employed by or serve as a consultant for BSD Medical. The laboratory portion of the study was performed by two authors (A.C.L., with 4 years of experience with bovine liver models; N.A.D., a student assistant).

Liver Procurement and Perfusion

Fresh, normal bovine livers and blood were obtained from a local slaughterhouse (G&C Packing, Colorado Springs, Colo). Livers underwent approximately 15 minutes of warm ischemia prior to excision and flushing with 10 L of chilled Krebs-Henseleit solution, which contained 30 000 USP units of heparin. Seven liters of blood was collected from each slaughtered cow; the blood was filtered for clots and particulates and mixed with 30 000 USP units of heparin. Both the liver and blood were iced to maintain hypothermia at 4°–6°C and were transported to our research laboratory. Total cold ischemic time averaged 2 hours.

Prior to the experiments, the livers were perfused with autologous blood by using a perfusion system (Fig 1). The main portal vein was cannulated by using a 24-F Foley catheter, which was connected to a centrifugal pump (Bio-Medicus Bio-Console, model 540; Medtronic, Minneapolis, Minn). The blood passed through a 500-mL bubble trap and a membrane oxygenator and heat exchanger (NT Affinity; Medtronic) that were connected to a canister of 95% oxygen and 5% carbon dioxide (Airgas, Radnor, Pa) to achieve

Published online before print
10.1148/radiol.12120486 **Content codes:** GI IR

Radiology 2013; 267:129–136

Abbreviations:
CI = confidence interval
LAD = long-axis diameter
MW = microwave
RF = radiofrequency
SAD = short-axis diameter

Author contributions:
Guarantors of integrity of entire study, G.D.D., A.C.L.; study concepts/study design or data acquisition or data analysis/interpretation, all authors; manuscript drafting or manuscript revision for important intellectual content, all authors; manuscript final version approval, all authors; literature research, G.D.D., N.A.D., A.C.L.; experimental studies, G.D.D., N.A.D., A.C.L.; statistical analysis, G.D.D., A.C.L., D.A.G.; and manuscript editing, G.D.D., N.A.D., A.C.L.

Conflicts of interest are listed at the end of this article.

Figure 1

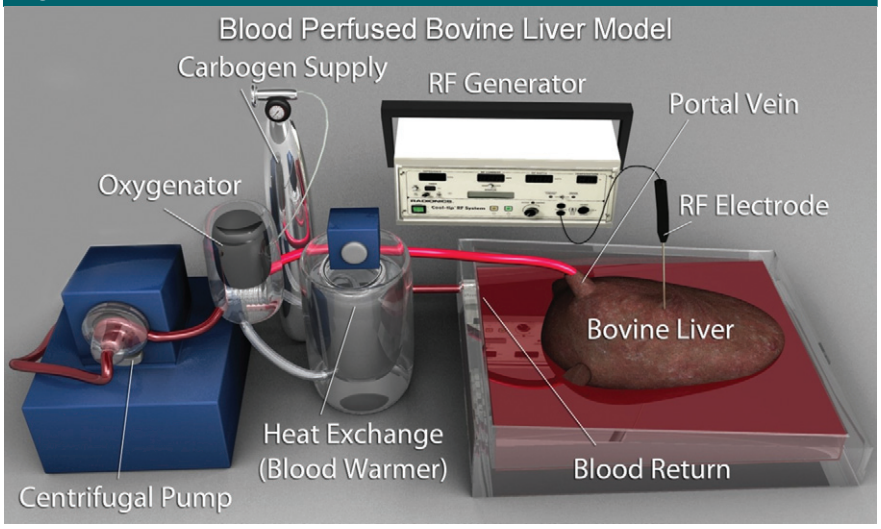

Figure 1: Computer-generated image shows components of the liver perfusion apparatus.

Figure 2

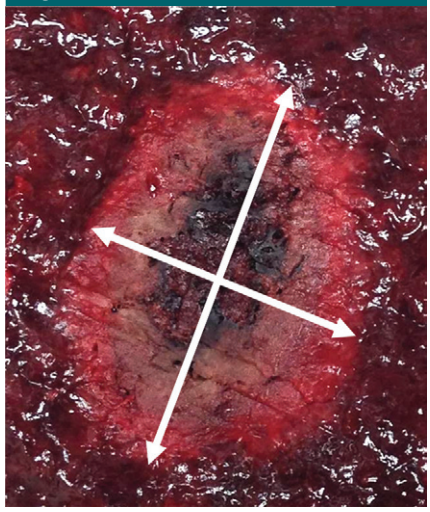

Figure 2: Ablation specimen shows the measurement technique for LAD (long arrow) and SAD (short arrow).

40%–50% oxygenation and a temperature of 37°C. The blood flow rate was controlled by the centrifugal pump and was monitored with a flowmeter (BioMedicus, model TX40; Medtronic). Flow rates were set at 60, 70, 80, 90, and 100 mL/min per 100 g of tissue to reflect normal portal venous flow rates in humans. Intrahepatic blood flow in the hepatic segments where ablations were to be performed was confirmed by using color Doppler ultrasonography (US) (IU 22, V6–2; Philips Healthcare, Andover, Mass).

RF and MW Ablation Equipment

One RF and one MW ablation system were used in the study. The RF ablation system was chosen on the basis of extensive prior experience with the device and its availability in our laboratory. The MW ablation system was chosen on the basis of the manufacturer's interest in supporting the study.

The RF ablation system (Cool-Tip; Covidien, Boulder, Colo) consisted of a 480-kHz 200-W alternating electric-current generator (model CC-1–117; Covidien), a 17-gauge 3.0-cm monopolar internally cooled applicator (model SWCT 1530; Covidien), a roller pump (model PE-PM; Covidien), and a dispersive electrode. This system was used to create all RF ablations. The applicators were cooled to 18°–22°C by internal perfusion with chilled normal saline by using the roller pump.

All MW ablations were created with a system (MicroThermX; BSD Medical) consisting of a 15-gauge single-needle applicator with a 5.0-cm antenna and integral shaft cooling system (SynchroWave, model SW-1415; BSD Medical) and a 915-MHz power generator (model MTX-180; BSD Medical) that operates at a maximum of 60 W per antenna. The antenna was perfused with a sterile isotonic saline solution with the temperature selection setting set to "normal" on the coolant pump.

Ablation Location and Technique

The bovine liver has lobar anatomy that is similar to the human liver, with large right and left lobes (40). RF and MW applicators were placed alternately in the anterior or posterior segment of the right lobe. US guidance was used to place the applicator tips at least 2 cm away from gray-scale visible portal or hepatic veins and at least 1 cm deep at the level of the hepatic capsule.

Sixty ablations (30 RF and 30 MW) were performed in 15 bovine livers. Of the 15 livers, three were perfused at each of the following portal flow rates: 60, 70, 80, 90, and 100 mL/min per 100 g. Four ablations were performed in each liver: two with RF and two with MW. By using the manufacturers' recommended clinical protocols, RF ablations were performed for 12 minutes in the impedance mode at the maximum power setting (200 W), and MW ablations were performed for 10 minutes at the maximum power setting (60 W). Immediately after each ablation, the RF or MW applicator was withdrawn, and a wooden marker probe was inserted into the track of the applicator.

Examination of the Ablation Specimens

On the basis of prior evidence of a close correlation between the histopathologic and gross assessment of the extent of coagulative necrosis in liver ablations, the size of ablations in this study was determined from measurement of the gross specimens (7,34,35,39,41) (Fig 2). After completion of all ablations in a liver, the liver was disconnected from the perfusion apparatus and dissected. The livers were sliced immediately adjacent and parallel to the marker probes in the applicator tracks, thus bisecting each ablation lesion. The maximum long-axis diameter (LAD) and short-axis diameter (SAD) of each ablation zone (outer margin to outer margin of the

Figure 3

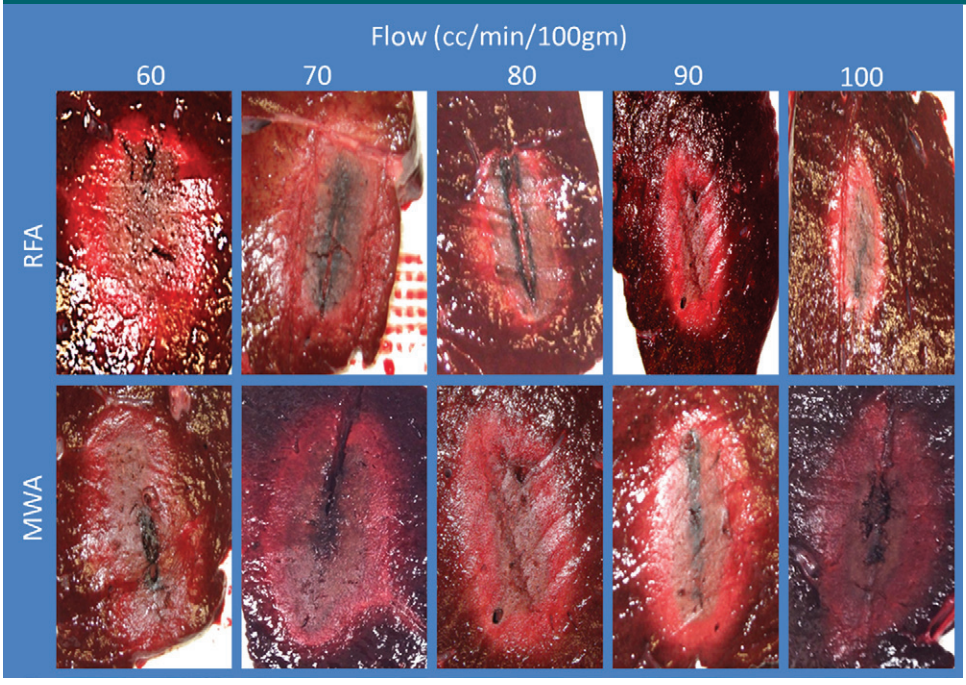

Figure 3: RF and MW ablation specimens for each of the portal venous flow rates from 60 to 100 mL/min per 100 g of hepatic tissue. Note the progressive decrease in size of the RF ablation lesions and the lack of change in the size of the MW ablation lesions (from left to right) as the flow rate increases. *MWA* = MW ablation, *RFA* = RF ablation.

red zone) were measured (Fig 2), and the volume *(V)* of the ablation zone was calculated by using the formula for an ellipsoid: $V = 4/3\pi \cdot (LAD/2)(SAD/2)(SAD/2)$.

Statistical Analysis

A backward stepwise model-fitting approach was used to examine the effect of location, ablation device, and actual flow rate on three outcomes: LAD, SAD, and volume. Residual diagnostics were used to examine goodness of fit (42). All calculations were done by using software (SAS/STAT, version 9.3; SAS Institute, Cary, NC).

Three general linear mixed models were fit, one for each outcome (LAD, SAD, and volume) (43). The fixed predictors included indicator variables for ablation device (RF or MW), location (anterior or posterior right lobe), and measures of actual flow rate in milliliters per minute per 100 g. The full model in every cell approach allowed different estimates of intercept and slope to be calculated for each ablation method according to lobe combination. The liver was fit as a random effect, with an unstructured covariance. Fitting a model with the location nested within the liver as a random effect was considered but lacked enough replicates within each location to allow convergence. At an α level of .05, the null hypothesis of no difference between the lines according to location was tested by using the Wald test with Kenward-Roger degrees of freedom (44).

Nonsignificance of the results led to a reduced model for the means. The fixed predictors were indicator variables for ablation device and measures of flow rate. A full model was fit in every cell, allowing different estimates of intercept and slope to be calculated for each ablation device. The null hypothesis of no difference between the lines according to ablation device was tested. A step-down test was used to describe the differences in slopes according to ablation device. Parameter estimates and 95% confidence intervals (CIs) were produced. Model-based *F* tests were reported by giving the statistic, the numerator degrees of freedom, the denominator degrees of freedom, and the *P* value.

A post hoc power analysis was performed by using the methods of Taylor and Muller (45) to account for the estimation of the means and variances before the power calculation. The power calculation is likely to be conservative, because it did not account for the fact that the power calculation was only done because the initial result was not significant (45).

Results

Sample pathologic specimens for the two devices at the different flow rates are shown in Figure 3. A total of 15 RF and 17 MW ablations were performed in the anterior right lobe, and 13 MW and 15 RF ablations were performed in the posterior right lobe. The means and standard deviations for the LAD, SAD, and volume of the RF and MW ablations are shown in the Table 1.

LAD

Ablation location was not a significant predictor of LAD ($F = 1.03$, numerator degrees of freedom = 4, denominator degrees of freedom = 52, $P = .4005$). In the reduced model, ablation device produced a significant difference in LAD ($F = 303.54$, numerator degrees of freedom = 2, denominator degrees of

Mean Measurements of Ablation Lesions at Various Portal Venous Flow Rates

Measure	60 mL/min per 100 g		70 mL/min per 100 g		80 mL/min per 100 g		90 mL/min per 100 g		100 mL/min per 100 g	
	RF	MW	RF	MW	RF	MW	RF	MW	RF	MW
LAD (cm)	3.23 ± 0.19	4.97 ± 0.48	3.32 ± 0.21	4.73 ± 0.21	2.83 ± 0.48	5.21 ± 0.44	2.78 ± 0.23	4.97 ± 0.29	2.62 ± 0.28	5.22 ± 0.17
SAD (cm)	2.72 ± 0.26	2.92 ± 0.18	2.12 ± 0.43	2.93 ± 0.10	1.88 ± 0.16	2.87 ± 0.15	1.88 ± 0.30	2.95 ± 0.12	1.63 ± 0.15	2.82 ± 0.12
Volume (cm^3)	12.54 ± 2.08	22.00 ± 1.45	8.00 ± 3.08	21.30 ± 0.95	5.41 ± 1.64	22.4 ± 1.63	5.31 ± 1.76	22.6 ± 1.53	3.72 ± 1.01	21.66 ± 1.29

Note.—Data are means ± standard deviations. Portal venous flow rates are 60 to 100 mL/min per 100 g of hepatic tissue. There were six ablations created with each device for every flow rate shown here.

Figure 4

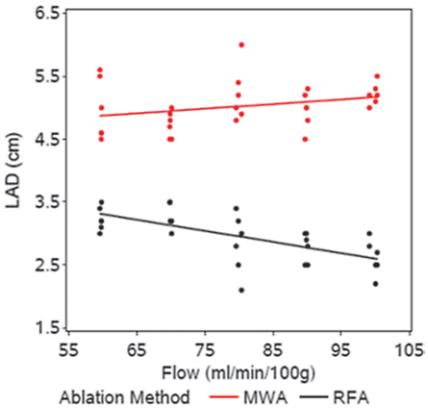

Figure 4: Graph shows LAD measurements for MW and RF ablation lesions with changes in portal venous flow. *MWA* = MW ablation, *RFA* = RF ablation.

Figure 5

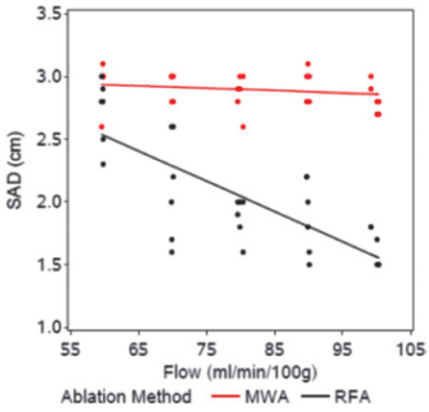

Figure 5: Graph shows SAD measurements for MW and RF ablation lesions with changes in portal venous flow. *MWA* = MW ablation, *RFA* = RF ablation.

freedom = 56, $P < .0001$). The slope of the relationship between flow rate and LAD was significantly different according to the ablation device used ($t = 4.20$, $df = 56$, $P < .0001$; 95% CI for the difference in slope between MW ablations and RF ablations: 0.013, 0.037).

The predicted regression lines were LAD = 4.4 + (0.007 · flow) for MW ablations and LAD = 4.4 − (0.018 · flow) for RF ablations. The slope for MW ablations was not significantly different from 0 (β = 0.007, standard error = 0.004, $t = 1.74$, $df = 56$, $P = .087$). For RF ablations, the mean LAD ablated did differ significantly according to flow rate, so that for an increase in flow of 1 mL/min per 100 g, the LAD ablated decreased by 0.018 cm (95% CI: −0.026, −0.009) (Fig 4).

SAD

Ablation location was not a significant predictor of SAD ($F = 0.77$, numerator degrees of freedom = 4, denominator degrees of freedom = 42.3, $P = .5509$). In the reduced model, the ablation device used produced a significant difference in SAD ($F = 143.81$, numerator degrees of freedom = 2, denominator degrees of freedom = 43, $P < .0001$). The slope of the relationship between flow rate and LAD was significantly different according to the ablation device used ($t = 5.90$, $df = 43$, $P < .0001$; 95% CI for the difference in slope between MW ablations and RF ablations: 0.014, 0.030).

The predicted regression lines were SAD = 3.05 − (0.002 · flow) for MW ablations and SAD = 3.97 − (0.024 · flow) for RF ablations. The slope for MW ablations was not significantly different from 0 (β = 0.002, standard error = 0.003, $t = -0.56$, $df = 26$, $P = .5836$). For RF ablations, the mean SAD ablated did differ significantly according to flow rate, so that for an increase in flow of 1 mL/min per 100 g, the SAD decreased by 0.02 cm (95% CI: −0.030, −0.017) (Fig 5).

Volume

Ablation location was not a significant predictor of the volume ablated ($F = 0.53$, numerator degrees of freedom = 4, denominator degrees of freedom = 43, $P = .7160$). In the reduced model, the ablation device used produced a significant difference in volume ($F = 601.3$, numerator degrees of freedom = 2, denominator degrees of freedom = 43, $P < .0001$). The slope of the relationship between flow rate and volume was significantly different according to the ablation device used ($t = 6.75$, $df = 43$, $P < .0001$; 95% CI for the difference in slope between MW ablations and RF ablations: 0.15, 0.27).

Figure 6

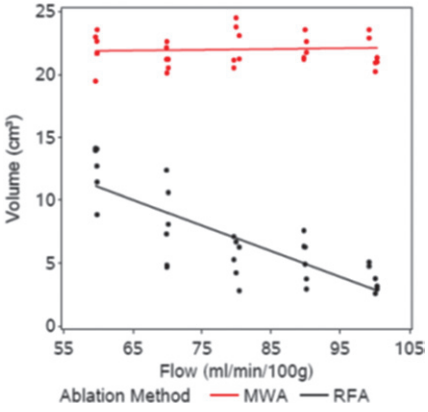

Figure 6: Graph shows volume measurements for MW and RF ablation lesions with changes in portal venous flow. *MWA* = MW ablation, *RFA* = RF ablation.

The predicted regression lines were volume = 21.5 + (0.006 · flow) for MW ablations and volume = 0.006 − (0.240 · flow) for RF ablations. The slope for MW ablations was not significantly different from 0 (β = 0.006, standard error = 0.025, t = 0.23, df = 28.7, P = .8229). For RF ablations, the mean volume ablated did differ significantly according to flow rate, so that for an increase in flow of 1 mL/min per 100 g, the volume ablated decreased by 0.2 cm^3 (95% CI: −0.26, 0.15) (Fig 6).

Results of the post hoc power analysis showed that the power for the hypothesis test of zero slope for the MW ablation was 0.057 (95% CI: 0.05, 1.00). The power analysis accounted for the fact that we used sample observed estimates of both the means and the variances, which accounts for the wide width of the 95% CI. Even conducting the study with 60 livers would still produce a power of only 0.082 (95% CI: 0.05, 1.00). Post hoc power would be even smaller for the outcomes of LAD and SAD and was not calculated.

Discussion

Predictability and reproducibility of the thermal lesions created by ablation devices are critical to the successful treatment of hepatic tumors (46). Not knowing how an ablation device is going to perform prevents appropriate treatment planning and can result in over- or undertreatment. Overtreatment, defined as destruction of tissue beyond the ablation of a tumor and the desired margin of normal tissue, can cause excessive destruction of adjacent normal hepatic tissue and potential injury to critical adjacent structures, such as bile ducts, diaphragm, and bowel (47,48). Undertreatment, which is the failure to eradicate all tumor, is a technical failure that could require immediate retreatment or result in a high local tumor failure rate. The variability of the size of coagulation necrosis produced with RF ablation systems suggests the need for an ablation system that can produce the same size of ablation for a given operational setting in all patients, irrespective of variations in hepatic perfusion or background hepatic pathologic condition (5–22).

Our results agree with those of previous reports of the susceptibility of RF ablation to variations in hepatic blood flow (8–22). We demonstrated a significant inverse linear correlation between changes in portal venous blood flow and the size of coagulation necrosis produced with RF ablation. The mean decrease in the SAD of RF ablation lesions from 60 to 100 mL/min per 100 g of portal venous blood flow was 1.1 cm (decrease from 2.7 cm to 1.6 cm). The mean decrease in lesion volume with RF ablation was a substantial 350% (decrease from 12.5 cm^3 to 3.7 cm^3). Because the flow rates in our study are within the spectrum of normal portal venous flow rates in humans, these results are likely clinically relevant (49). The potential importance of this variability is clear in a hypothetical clinical scenario of a patient with a 2-cm hepatic tumor: While a single 2.7-cm ablation might be adequate to eradicate the tumor, a single 1.6-cm ablation would likely fail to destroy the entire tumor. This level of variability and uncertainty in outcome in terms of patient care is unacceptable.

On the other hand, our MW ablation results did not demonstrate a significant change in the average LAD, SAD, and volume of MW ablation lesions from 60 to 100 mL/min per 100 g of portal venous blood flow. This indicates one of two things: either the mean size of MW ablations does not change with different flow rates, or our study had insufficient power to demonstrate a small change in the mean size of the MW ablations. Nonetheless, even if our study failed to demonstrate a small change in the size of MW ablations, Figures 4–6 depict the marked difference between the susceptibility of RF and MW techniques to changes in portal venous blood flow. By applying our MW ablation results to the same hypothetical clinical scenario of a patient with a 2-cm tumor, a single predictable and reproducible 2.8-cm ablation would likely eradicate the tumor across the full physiologic range of portal venous blood flow.

The difference in susceptibility of RF and MW ablation to alterations in hepatic blood flow is not unexpected from a physics perspective. RF operates at a low electromagnetic frequency (500 kHz) and has a long wavelength (9 m). During ablation, alternating RF current passes between the applicator and the grounding pad and heats tissue around the applicator by means of ionic agitation and frictional heat. The amount of frictional heat is directly related to the conductivity of the tissue through which the current passes (low conductivity = more heat; high conductivity = less heat). The RF conductivity of hepatic tissue is five times less than that of blood; thus, as blood flow increases, it provides an alternate low-resistance pathway for the RF current, which diminishes the amount of frictional heat around the applicator and results in a smaller thermal lesion. MW ablation operates at a much higher frequency and shorter wavelength (915 MHz and 5 cm, as used in the present study) and heats tissue by tumbling the water molecules immediately adjacent to the applicator. The difference in MW conductivity of hepatic tissue and blood is only twofold; thus, variation in blood flow has less of an effect on the size of a thermal lesion than that seen with RF ablation (50,51).

Our study had several limitations. Most important, we evaluated only one RF ablation device and one MW ablation device, each operated with a specific

ablation protocol; therefore, it is unknown if the difference in susceptibility to variations in portal blood flow will be found with other devices or even with the same devices operated with different generator settings or lengths of ablation time. We designed our study to avoid large hepatic blood vessels and assess the effect of variation of global hepatic perfusion on the overall size of RF and MW ablations; thus, we cannot comment on the effect of variation in hepatic blood flow on the local heat sink effect of adjacent large blood vessels in terms of ablation size or configuration.

The perfused bovine liver model has several intrinsic limitations. We did not perfuse the hepatic artery, as it is technically challenging in the bovine liver, owing to a small artery. While this would clearly have had an additional negative effect on the size of RF ablations, we suspect that there would not have been any effect of the size of MW ablations; however, this remains to be proved with future study (14,15). In addition, the bovine liver model represents normal noncirrhotic liver tissue and lacks the presence of tumor; thus, it may be difficult to extrapolate our findings to patients with cirrhosis and those with tumors, either with or without cirrhosis. However, we believe that our results are clinically relevant, given the need to ablate both a tumor and the safety margin of surrounding nontumoral hepatic parenchyma. As shown in the article by Montgomery et al, the performance of RF ablation devices in tumors smaller than 2.25 cm in diameter is unrelated to tumor type or size or the presence or absence of cirrhosis and is most likely controlled by hepatic perfusion (23). Thus, we believe that knowledge about the performance of RF and MW ablation devices in the bovine liver model is likely translatable to patients who have primary or secondary hepatic tumors, either with or without cirrhosis. Last, our study shares a recently identified limitation of the measurement of ablation lesions in gross pathologic specimens. Brace et al (52) reported that there is variable shrinkage of liver tissue with RF and MW ablation and that the gross measurement of the coagulative necrosis in dissected specimens may lead to underestimation of the true volume of the ablated tissue.

In conclusion, we have demonstrated a significant difference in the susceptibility of RF and MW ablation devices to changes in portal venous blood flow within the range of normal physiologic flow rates. The size of RF ablation lesions is highly variable, with a significant inverse relationship to the rate of portal venous blood flow; conversely, the size of MW ablation lesions is unaffected by changes in portal venous blood flow. This observation could have a substantial effect on the clinical decision of which ablation devices should be used to treat patients with hepatic tumors. The availability of a device that creates a predictable and reproducible size of coagulation necrosis in all patients could extend the range of tumors and patients who can be treated effectively with ablation therapy.

Disclosures of Conflicts of Interest: G.D.D. Financial activities related to the present article: ablation equipment and study funding from BSD Medical. Financial activities not related to the present article: author is consultant for Philips Research. Other relationships: none to disclose. **N.A.D.** Financial activities related to the present article: ablation equipment and study funding from BSD Medical. Financial activities not related to the present article: none to disclose. Other relationships: none to disclose. **A.C.L.** Financial activities related to the present article: n ablation equipment and study funding from BSD Medical. Financial activities not related to the present article: none to disclose. Other relationships: none to disclose. **D.A.G.** No relevant conflicts of interest to disclose.

References

1. Lencioni R, Crocetti L, Cioni D, Della Pina C, Bartolozzi C. Percutaneous radiofrequency ablation of hepatic colorectal metastases: technique, indications, results, and new promises. Invest Radiol 2004;39(11):689–697.
2. Wong SL, Mangu PB, Choti MA, et al. American Society of Clinical Oncology 2009 clinical evidence review on radiofrequency ablation of hepatic metastases from colorectal cancer. J Clin Oncol 2010;28(3):493–508.
3. Solbiati L, Ierace T, Goldberg SN, et al. Percutaneous US-guided radio-frequency tissue ablation of liver metastases: treatment and follow-up in 16 patients. Radiology 1997;202(1):195–203.
4. Livraghi T, Goldberg SN, Lazzaroni S, et al. Hepatocellular carcinoma: radio-frequency ablation of medium and large lesions. Radiology 2000;214(3):761–768.
5. Hori T, Nagata K, Hasuike S, et al. Risk factors for the local recurrence of hepatocellular carcinoma after a single session of percutaneous radiofrequency ablation. J Gastroenterol 2003;38(10):977–981.
6. Choi D, Lim HK, Rhim H, et al. Percutaneous radiofrequency ablation for early-stage hepatocellular carcinoma as a first-line treatment: long-term results and prognostic factors in a large single-institution series. Eur Radiol 2007;17(3):684–692.
7. Lu DS, Yu NC, Raman SS, et al. Radiofrequency ablation of hepatocellular carcinoma: treatment success as defined by histologic examination of the explanted liver. Radiology 2005;234(3):954–960.
8. Mulier S, Ni Y, Miao Y, et al. Size and geometry of hepatic radiofrequency lesions. Eur J Surg Oncol 2003;29(10):867–878.
9. Ahmed M, Liu Z, Humphries S, Goldberg SN. Computer modeling of the combined effects of perfusion, electrical conductivity, and thermal conductivity on tissue heating patterns in radiofrequency tumor ablation. Int J Hyperthermia 2008;24(7):577–588.
10. Liu Z, Ahmed M, Sabir A, Humphries S, Goldberg SN. Computer modeling of the effect of perfusion on heating patterns in radiofrequency tumor ablation. Int J Hyperthermia 2007;23(1):49–58.
11. Patterson EJ, Scudamore CH, Owen DA, Nagy AG, Buczkowski AK. Radiofrequency ablation of porcine liver in vivo: effects of blood flow and treatment time on lesion size. Ann Surg 1998;227(4):559–565.
12. de Baere T, Bessoud B, Dromain C, et al. Percutaneous radiofrequency ablation of hepatic tumors during temporary venous occlusion. AJR Am J Roentgenol 2002;178(1):53–59.
13. Washburn WK, Dodd GD 3rd, Kohlmeier RE, et al. Radiofrequency tissue ablation: effect of hepatic blood flow occlusion on thermal injuries produced in cirrhotic livers. Ann Surg Oncol 2003;10(7):773–777.
14. Chinn SB, Lee FT Jr, Kennedy GD, et al. Effect of vascular occlusion on radiofrequency ablation of the liver: results in a porcine model. AJR Am J Roentgenol 2001;176(3):789–795.
15. Ritz JP, Lehmann K, Isbert C, Roggan A, Germer CT, Buhr HJ. Effectivity of laser-induced thermotherapy: in vivo comparison of arterial microembolization and complete hepatic inflow occlusion. Lasers Surg Med 2005;36(3):238–244.
16. Chang CK, Hendy MP, Smith JM, Recht MH, Welling RE. Radiofrequency ablation of the porcine liver with complete hepatic vas-

cular occlusion. Ann Surg Oncol 2002;9(6):594–598.

17. Shen P, Fleming S, Westcott C, Challa V. Laparoscopic radiofrequency ablation of the liver in proximity to major vasculature: effect of the Pringle maneuver. J Surg Oncol 2003;83(1):36–41.
18. Wacker FK, Reither K, Ritz JP, Roggan A, Germer CT, Wolf KJ. MR-guided interstitial laser-induced thermotherapy of hepatic metastasis combined with arterial blood flow reduction: technique and first clinical results in an open MR system. J Magn Reson Imaging 2001;13(1):31–36.
19. Iwamoto T, Kawai N, Sato M, et al. Effectiveness of hepatic arterial embolization on radiofrequency ablation volume in a swine model: relationship to portal venous flow and liver parenchymal pressure. J Vasc Interv Radiol 2008;19(11):1646–1651.
20. Goldberg SN, Hahn PF, Halpern EF, Fogle RM, Gazelle GS. Radio-frequency tissue ablation: effect of pharmacologic modulation of blood flow on coagulation diameter. Radiology 1998;209(3):761–767.
21. Goldberg SN, Gazelle GS, Dawson SL, Rittman WJ, Mueller PR, Rosenthal DI. Tissue ablation with radiofrequency: effect of probe size, gauge, duration, and temperature on lesion volume. Acad Radiol 1995;2(5):399–404.
22. Bitsch RG, Düx M, Helmberger T, Lubienski A. Effects of vascular perfusion on coagulation size in radiofrequency ablation of ex vivo perfused bovine livers. Invest Radiol 2006;41(4):422–427.
23. Montgomery RS, Rahal A, Dodd GD 3rd, Leyendecker JR, Hubbard LG. Radiofrequency ablation of hepatic tumors: variability of lesion size using a single ablation device. AJR Am J Roentgenol 2004;182(3):657–661.
24. Goldberg SN, Solbiati L, Hahn PF, et al. Large-volume tissue ablation with radio frequency by using a clustered, internally cooled electrode technique: laboratory and clinical experience in liver metastases. Radiology 1998;209(2):371–379.
25. Bradley SE, Ingelfinger FJ, Bradley GP, Curry JJ. The estimation of hepatic blood flow in man. J Clin Invest 1945;24(6):890–897.
26. Moreno AH, Burchell AR, Rousselot LM, Panke WF, Slafsky F, Burke JH. Portal blood flow in cirrhosis of the liver. J Clin Invest 1967;46(3):436–445.
27. Daneshmend TK, Jackson L, Roberts CJC. Physiological and pharmacological variability in estimated hepatic blood flow in man. Br J Clin Pharmacol 1981;11(5):491–496.
28. Wright AS, Sampson LA, Warner TF, Mahvi DM, Lee FT Jr. Radiofrequency versus microwave ablation in a hepatic porcine model. Radiology 2005;236(1):132–139.
29. Simon CJ, Dupuy DE, Iannitti DA, et al. Intraoperative triple antenna hepatic microwave ablation. AJR Am J Roentgenol 2006;187(4):W333–W340.
30. Garrean S, Hering J, Saied A, et al. Ultrasound monitoring of a novel microwave ablation (MWA) device in porcine liver: lessons learned and phenomena observed on ablative effects near major intrahepatic vessels. J Gastrointest Surg 2009;13(2):334–340.
31. Yu NC, Raman SS, Kim YJ, Lassman C, Chang X, Lu DS. Microwave liver ablation: influence of hepatic vein size on heat-sink effect in a porcine model. J Vasc Interv Radiol 2008;19(7):1087–1092.
32. Brace CL, Laeseke PF, Sampson LA, Frey TM, van der Weide DW, Lee FT Jr. Microwave ablation with a single small-gauge triaxial antenna: in vivo porcine liver model. Radiology 2007;242(2):435–440.
33. Brace CL, Laeseke PF, Sampson LA, Frey TM, van der Weide DW, Lee FT Jr. Microwave ablation with multiple simultaneously powered small-gauge triaxial antennas: results from an in vivo swine liver model. Radiology 2007;244(1):151–156.
34. Awad MM, Devgan L, Kamel IR, Torbensen M, Choti MA. Microwave ablation in a hepatic porcine model: correlation of CT and histopathologic findings. HPB (Oxford) 2007;9(5):357–362.
35. Gravante G, Ong SL, Metcalfe MS, Strickland A, Dennison AR, Lloyd DM. Hepatic microwave ablation: a review of the histological changes following thermal damage. Liver Int 2008;28(7):911–921.
36. Hines-Peralta AU, Pirani N, Clegg P, et al. Microwave ablation: results with a 2.45-GHz applicator in ex vivo bovine and in vivo porcine liver. Radiology 2006;239(1):94–102.
37. Shibata T, Niinobu T, Ogata N. Comparison of the effects of in-vivo thermal ablation of pig liver by microwave and radiofrequency coagulation. J Hepatobiliary Pancreat Surg 2000;7(6):592–598.
38. Sommer CM, Koch V, Pap B, et al. Effect of tissue perfusion on microwave ablation: experimental in vivo study in porcine kidneys. J Vasc Interv Radiol 2011;22(12):1751–1757.
39. Orsi MD, Dodd GD 3rd, Cardan RA, et al. In vitro blood-perfused bovine liver model: a physiologic model for evaluation of the performance of radiofrequency ablation devices. J Vasc Interv Radiol 2011;22(10):1478–1483.
40. Budras KD, Habel RE. Bovine liver anatomy: an illustrated text. Hanover, Germany: Schlutersche GmbH & Co, 2003; 74–75.
41. Burns SK, Dodd GD 3rd, McManus LM, et al. 3T magnetic resonance imaging accurately depicts radiofrequency ablation zones in a blood-perfused bovine liver model. J Vasc Interv Radiol 2012;23(6):801–808.
42. Laird NM, Ware JH. Random-effects models for longitudinal data. Biometrics 1982;38(4):963–974.
43. Muller KE, Fetterman BA. Regression and ANOVA: an integrated approach using SAS software. Cary, NC: SAS Institute/Wiley, 2003.
44. Kenward MG, Roger JH. Small sample inference for fixed effects from restricted maximum likelihood. Biometrics 1997;53(3):983–997.
45. Taylor DJ, Muller KE. Bias in linear model power and sample size calculation due to estimating noncentrality. Commun Stat Theory Methods 1996;25(7):1595–1610.
46. Dodd GD 3rd, Frank MS, Aribandi M, Chopra S, Chintapalli KN. Radiofrequency thermal ablation: computer analysis of the size of the thermal injury created by overlapping ablations. AJR Am J Roentgenol 2001;177(4):777–782.
47. Livraghi T, Solbiati L, Meloni MF, Gazelle GS, Halpern EF, Goldberg SN. Treatment of focal liver tumors with percutaneous radio-frequency ablation: complications encountered in a multicenter study. Radiology 2003;226(2):441–451.
48. Liang P, Wang Y, Yu X, Dong B. Malignant liver tumors: treatment with percutaneous microwave ablation—complications among cohort of 1136 patients. Radiology 2009;251(3):933–940.
49. Sherriff SB, Smart RC, Taylor I. Clinical study of liver blood flow in man measured by 133Xe clearance after portal vein injection. Gut 1977;18(12):1027–1031.
50. Gabriel C, Gabriel S. Compilation of the dielectric properties of body tissues at RF and MW frequencies. http://www.brooks.af.mil/AFRL/HED/hedr/reports/dielectric/home.html (authorized mirror at http://niremf.ifac.cnr.it/docs/DIELECTRIC/home.html). Accessed June 20, 2012.
51. Gabriel C. Compilation of the dielectric properties of body tissues at RF and microwave frequencies. Report N.AL/OE-TR-1996-0037, Occupational and environmental health directorate, Radiofrequency Radiation Division, Brooks Air Force Base, Texas (USA), June 1996.
52. Brace CL, Diaz TA, Hinshaw JL, Lee FT Jr. Tissue contraction caused by radiofrequency and microwave ablation: a laboratory study in liver and lung. J Vasc Interv Radiol 2010;21(8):1280–1286.